

## EFFECT OF ABRUPT PRESSURE GRADIENTS ON THE STRUCTURE OF TURBULENT BOUNDARY LAYERS

Promode R. BANDYOPADHYAY

Mail Stop 163, NASA Langley Research Center  
Hampton, VA 23665-5225  
USA

### ABSTRACT

The structure of a turbulent boundary-layer due to abruptly applied strong favorable and adverse pressure gradients, leading to relaminarization and separation, respectively is considered. Digital image enhancement techniques have been applied to laser light sheet smoke flow visualization pictures. A 'local range modification' technique has been used to extract structural details otherwise lying ill-defined in the fully turbulent core. The cross-stream sections immediately prior to separation, and particularly those shortly after the application of the favorable pressure gradient, are vividly organized; there exists a criss-cross pattern in the spanwise plane with a mean orientation at about  $\pm 45^\circ$  to the vertical.

### INTRODUCTION

It is known that the structure of a turbulent boundary layer is Reynolds number dependent (Head and Bandyopadhyay 1981). The most striking aspect of this dependence is the increase in the aspect ratio of the hairpin vortices with Reynolds number. This can be viewed as an increasing effect of vortex stretching with Reynolds number. Once the hairpin vortices are formed, inviscid mechanisms govern their stretching (Bandyopadhyay 1980 and Perry and Chong 1982). So, much can be learnt about the structure of high Reynolds number turbulent boundary layers, without actually doing any high Reynolds number experiment which is resource intensive, by somehow enhancing the stretching of the hairpin vortices characteristic of low Reynolds numbers. Such an enhancement can be materialized by pressure gradients and the present work can be said to be doing just that.

An experimental investigation into the structure of turbulent boundary layers abruptly subjected to a favorable or adverse pressure gradient, leading to relaminarization or separation, respectively has been carried out. A spanwise organization of the hairpin vortices has been observed in all pressure gradients including that at zero. A more detailed account appears elsewhere (Bandyopadhyay 1989) where it is further shown that these observations are consistent with a double helix spiralling of the hairpin vortices. Only a brief account of the observation on the spanwise organization is given in the following.

### EXPERIMENTS

The experiments were carried out in the Low Speed Smoke Tunnel of the Cambridge University Engineering Department about ten to fifteen years ago. But, the flow

visualization could not be analyzed properly for a long time because, the hairpin vortex description of a turbulent boundary layer was neither developed nor widely accepted.

The distributions of the non-dimensional pressure gradient parameter,  $K(= (\nu/U_\infty^2)(dU_\infty/dx))$  computed using the measured static pressure distributions are shown in Fig. 1. The structure of turbulence has been found to depend on the sign of  $dK/dx$  (Bandyopadhyay 1989). The figures also include the locations where flow visualization has been carried out.

The computed distributions of the boundary layer integral quantities viz., momentum thickness Reynolds number  $Re_\theta$ , shape factor,  $H$ , local skin-friction  $c_f$  and boundary layer thickness  $\delta$ , are shown in Figs. 2 and 3. The figures also include several measured values. Note the failure of the turbulence model near separation and relaminarization. As possible clues to this, the physical aspects lacking in contemporary models are discussed in Bandyopadhyay (1989).

### RESULTS

Figure 4 shows a longitudinal section through the turbulent boundary layer abruptly subjected to a favorable pressure gradient. Note the rapid reduction in the boundary layer cross-sectional area.

Figure 5 shows cross-stream views shortly after the abrupt application of the favorable pressure gradient at the upstream location marked in Fig. 4. Figure 5(a) is an unprocessed image and Fig. 5(b) is the same image after L(ocal) R(ange) M(odification) and other digital edge enhancement like convolving and contouring. In Fig. 5b, note the criss-cross pattern at about  $\pm 45^\circ$  to the vertical. The pattern is vividly organized and two-dimensional in the spatial mean.

Figure 6 shows another cross-stream view (enhanced image but without LRM) of the favorable case shown in Fig. 5. Here, note the presence of the hairpin vortex cross-sections at the rotational/irrotational flow interface with their inner induced flow inclined at  $\pm 45^\circ$  to the vertical.

Figure 7 shows an enhanced cross-stream view of the turbulent boundary layer immediately prior to separation. Note the presence of a finer criss-cross pattern at about  $\pm 45^\circ$  to the vertical but, in only part of the cross-section — in the lower right area of the diagonal line extending from the mid-floor to the right edge of the layer.

Figure 8 shows an LRM and edge enhanced cross-stream view of a zero pressure gradient boundary layer at



$Re_\theta = 1700$ . However, note that this view was obtained with a light plane inclined upstream at  $45^\circ$  to the flow direction whereas, Figs. 5 to 7 were obtained with a light plane normal to the wall. Note that there is still a criss-cross pattern at  $\pm 45^\circ$  to the vertical but it is by no means as organized as in the pressure gradient flows. Elsewhere (Bandyopadhyay 1989) it is discussed in greater detail that in a turbulent boundary layer, the vorticity in the two legs of a hairpin vortex is usually not of the same magnitude. This causes a weak-strong interaction between the two legs. Due to stretching, the interaction leads to the spiralling of the hairpin vortex. Figure 9 shows a schematic representation of such a double helix spiralling of a hairpin vortex. A direct evidence of the existence of such a double helix pattern is given in Fig. 10.

Figure 10 shows a time sequence of cross-stream views of a zero pressure gradient turbulent boundary layer obtained with a light plane inclined upstream at  $45^\circ$  to the flow direction. Note the double helix spiralling of the marked hairpin cross-section in the outer part of the boundary layer. As time increases, the cross-section of the pair moves closer to the wall while at the same time the direction of the induced flow changes from the vertical to the horizontal (covering a phase of  $\pi/2$  of the double helix in Fig. 9). Thereafter, it becomes difficult to track the pair any further.

Figure 11 shows a schematic representation of the Reynolds number effect on the cross-stream criss-cross pattern. This takes into account the fact that, with increasing Reynolds number, there are more hairpin vortices per

unit floor area. The finer criss-cross pattern in the separating flow is consistent with the higher  $Re_\theta$  near separation (Fig. 3). The spanwise turbulence flux is a feature of the criss-cross pattern.

#### CONCLUSION

The present work shows some of the organized nature of the spanwise flow. It is concluded that there exists a criss-cross pattern at  $\pm 45^\circ$  to the vertical in turbulent boundary layers at all pressure gradients.

#### REFERENCES

BANDYOPADHYAY, P. R. (1980) Large structure with a characteristic upstream interface in turbulent boundary layers, *Phys. Fl.*, V23, No. 11, p. 2326.

BANDYOPADHYAY, P. R. (1989) The structure of relaminarizing and separating turbulent boundary layers, (subjudice).

HEAD, M. R. and Bandyopadhyay, P. (1981) New aspects of the structure of turbulent boundary layers, *J. Fluid Mech.*, V107, pp. 297-338.

PERRY, A. E. and Chong, M. S. (1982) On the mechanism of wall turbulence, *J. Fluid Mech.*, V119, pp. 173-217.

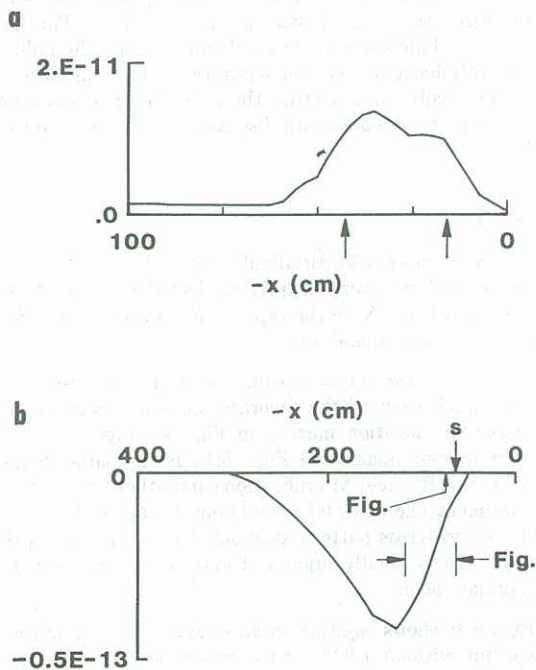


Figure 1. Pressure gradient parameter in the favorable (a) and adverse (b) pressure gradient experiments. The ordinate is proportional to  $K$ . The mean separation location is indicated by  $S$ .

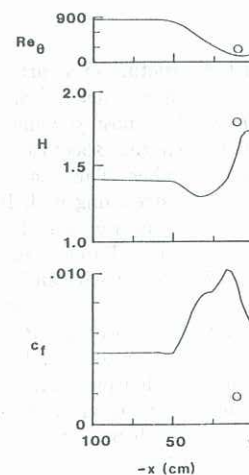


Figure 2. Computed development of the favorable pressure gradient boundary layer compared with measurements at the relaminarizing station.

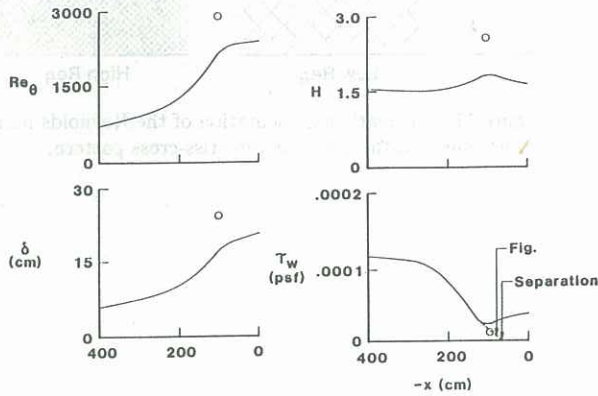


Figure 3. Computed development of the adverse pressure gradient boundary layer compared with measurements immediately prior to separation.

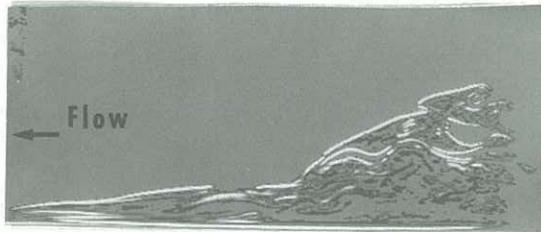


Figure 4. A longitudinal section through the turbulent boundary layer abruptly subjected to a favorable pressure gradient.

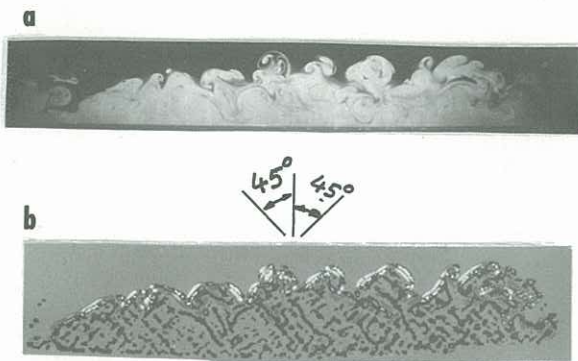


Figure 5. Cross-stream views shortly after the abrupt application of the favorable pressure gradient at the location marked in Fig. 4; (a) unprocessed image; (b) same image after LRM and other digital enhancement. Note the criss-cross pattern at about  $\pm 45^\circ$  to the vertical.



Figure 6. Another cross-stream view (enhanced image but without LRM) of the favorable station shown in Fig. 5.

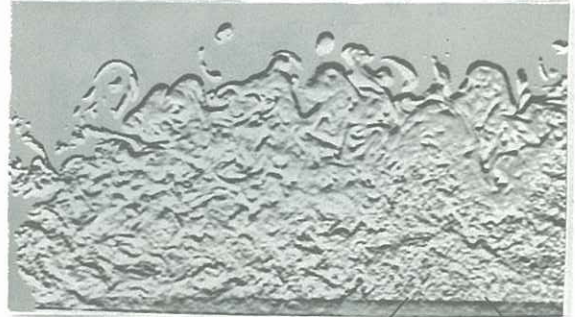


Figure 7. An enhanced cross-stream view of the turbulent boundary layer immediately prior to separation.

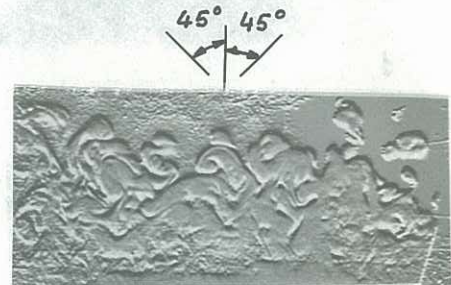


Figure 8. An enhanced cross-stream view of a zero pressure gradient boundary layer obtained with a light plane inclined upstream at  $45^\circ$  to the flow direction.

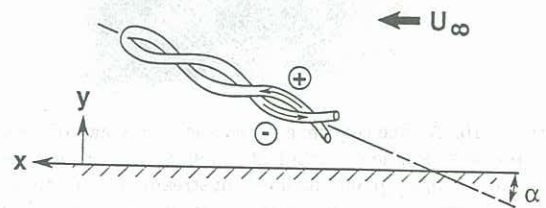


Figure 9. Schematic representation of the double helix spiralling of a hairpin vortex.



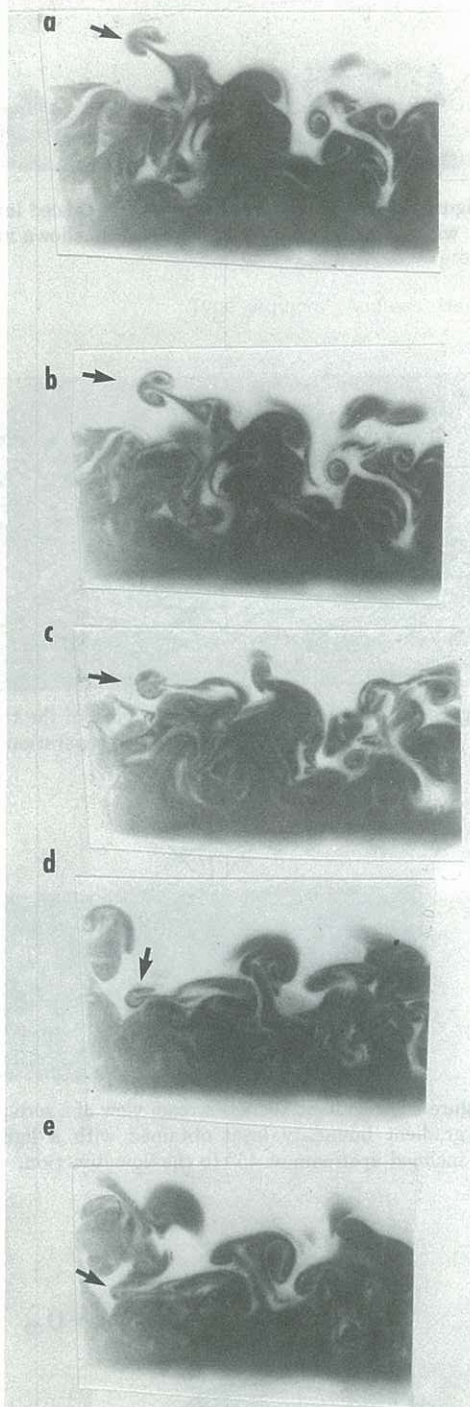


Figure 10. A time sequence of cross-stream views of a zero pressure gradient turbulent boundary layer obtained with a light plane inclined upstream at  $45^\circ$  to the flow direction. Time increases from (a) to (e). Note the double helix spiralling of the marked hairpin cross-section.

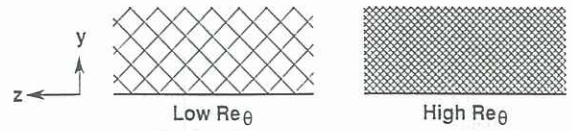


Figure 11. Schematic representation of the Reynolds number effect on the cross-stream criss-cross pattern.